ELSEVIER

Journal of Molecular Catalysis A: Chemical 175 (2001) 189–204

JOURNAL OF MOLECULAR CATALYSIS A: CHEMICAL

www.elsevier.com/locate/molcata

Metal–support interactions in cobalt-aluminum co-precipitated catalysts: XPS and CO adsorption studies

Alexander A. Khassin*, Tamara M. Yurieva, Vasiliy V. Kaichev, Valerii I. Bukhtiyarov, Anna A. Budneva, Evgeniy A. Paukshtis, Valentin N. Parmon

Boreskov Institute of Catalysis, 5, Pr. Lavrentieva, Novosibirsk 630090, Russia

Received 23 February 2001; received in revised form 28 March 2001; accepted 5 May 2001

Abstract

Cobalt-aluminum catalysts were prepared using either the precipitation of Co^{2+} in the presence of freshly prepared Zn-Al hydrotalcite (the promoted sample) or the co-precipitation of Co^{2+} and Al^{3+} (the unpromoted samples). The evolution of the initial hydrotalcite-like structure was monitored during its calcination and the reductive treatment by means of XPS. It was shown that at 480°C the reduction of the calcined samples results in the formation of Co^0 species, the further reduction at 650°C results in an increase of the amount of the Co^0 species. The samples reduced at 650°C chemisorb readily carbon monoxide at 77 K, while the sample reduced at 480°C does not chemisorb CO at 77 K. At elevated temperatures, all reduced samples are found to be able to chemisorb CO. Terminal CO moieties as well as monodentate carbonates, formates and carboxyl species were detected at the surface of the reduced samples at their exposure to the CO medium at the elevated temperature. The intensity of the IR absorption bands of chemisorbed CO are found proportional to the surface fraction of the Co^0 species, measured by XPS. The apparent red shift of the IR absorption bands is observed for CO adsorbed on the samples reduced at 480°C. The obtained data correlate with the catalytic properties of the Co-Al samples in hydrogenation reactions. The conclusion on the existence of a strong metal–support interaction in the samples under the study is made.

Keywords: Cobalt; Alumina; XPS; Carbon monoxide; Metal–support interaction

1. Introduction

Cobalt-alumina catalyst are well known to be highly active in hydrogenation reactions, e.g. of CO to hydrocarbons (the Fischer–Tropsch synthesis, FTS). Studies on the properties of these catalysts in the FTS are numerous [1–6].

Some studies report on a sufficient metal–support interaction for the Co-Al catalysts. For example, the Co^0 particles of some sol–gel prepared Co-Al catalysts appear to be inactive in the CO oxidation [7] at the temperatures <300°C, while impregnated Co/Al_2O_3 samples revealed high activity in this reaction already at 150–200°C. The temperature increase up to ca. 300°C leads to an increase of the catalyst activity of the sol–gel catalyst up to the values, which are characteristic for a conventional metallic cobalt. In [8], the reaction of the H_2–D_2 exchange over an Co-Al intermetallic compound, which is transformed to Co^0/Al_2O_3 during its activation, was found to be very slow at temperature <100°C, in spite of the adsorption of hydrogen over the metallic cobalt is

* Corresponding author. Tel.: +7-383-2-344109; fax: +7-383-2-343056.
E-mail address: a.a.khassin@catalysis.nsk.su (A.A. Khassin).

1381-1169/01/$ – see front matter
PII: S1381-1169(01)00216-3

known to proceed dissociatively. The activity in the deuterium exchange of the discussed Co-Al catalyst increases dramatically at ca. 200°C.

In the papers [7,8], the authors ascribed the observed difference in the catalytic properties to the existence of a sufficient metal–support interaction between Co and Al-containing oxide. At the moment, the actual nature of the proposed influence of the support on the catalytic properties of the Co^0 phase is not well studied and recognized.

Recently, we showed an effect of the catalyst reduction temperature on the activity and selectivity of the precipitated Co-Al catalyst in the CO hydrogenation [9]. The catalysts reduced at 480°C were found much less active and, simultaneously, much more selective to the olefin formation.

Here, we present the X-ray photoelectron spectroscopy (XPS) study of the same model Co-Al precipitated catalysts in respect to their evolution during the activation, as well as the FTIR data on the CO molecules adsorbed at temperatures from 77 to 527 K. The main focus of the study is the effect of the reduction temperature on the state of the catalyst and its active component and on the nature of the CO adsorption.

2. Experimental

2.1. Preparation of the catalysts

Two series of samples were used as objects for this study. Initial sample of Co-Al series (CA) with Co/Al atomic ratio of 1 was prepared by coprecipitation of Co^{2+} and Al^{3+}. Similar sample of Co-Zn-Al series (PZA) with atomic ratio of Co:Zn:Al = 1:1:2 was prepared by precipitation of Co^{2+} cations in the presence of a freshly coprecipitated Zn-Al support. All the precipitation procedures were performed from stoichiometric 10 wt.% aqueous solutions of the corresponding nitrates ('pure for chemical analysis' grade, Uralian plant of chemicals, Russia) at 60–70°C. The 7.5 wt.% water solution of Na_2CO_3 or that of NH_4HCO_3 were used as the precipitant. The precipitated catalysts were washed thoroughly by distilled water and dried overnight by an IR lamp in air. The detailed information on the way of the catalyst preparation and the results of the sample characterization was reported elsewhere (see [9], samples CA-II and P/ZA, correspondingly).

Below, we denote the uncalcined samples as CA-U and PZA-U, the samples after their calcination in the flowing Ar at 500°C for 2 h as CA-C and PZA-C, the calcined samples after their reduction in the flowing hydrogen at 480°C for 2 h — as CA-LT and PZA-LT, and those sample after their reduction at 650°C for 2 h — as CA-HT and PZA-HT.

2.2. Characterization techniques

The XPS measurements were performed using a VG ESCALAB HP spectrometer with non-monochromatized Al Kα radiation ($h\nu$ = 1486.6 eV). All spectra were taken in constant analyzer energy (10 eV) regime with resolution of about 1 eV. Before measurements the spectrometer was calibrated against Au $4f_{7/2}$ peak with binding energy (BE) of 84.0 eV and Cu $2p_{3/2}$ peak with BE = 932.6 eV. The shift caused by the charging effect has been corrected using the internal standard method, with C 1s peak at 284.8 eV from hydrocarbon contaminations being used as the reference. The samples were carefully mounted on a sample holder by means of a double-sided adhesive tape. The sample loading was performed in argon flow in order to avoid the contact of the sample with the air.

To extract the information about chemical states of the elements to be in interest, narrow regions of their core level spectra have been analyzed, original XPS spectra being deconvoluted on separate components. The latter procedure involved linear background subtraction and a curve-fitting using a mixed Gaussian–Lorentzian function. The reproducibility of the peak position was ±0.1 eV. The quantitative analysis was based on the areas of the XPS peaks, which was corrected on the atomic sensitivity factor of the corresponding elements [10]. Note that the use of the Al Kα radiation caused overlapping of the Co $2p_{3/2}$ spectral region with the Co $L_3M_{23}M_{45}$ Auger line. As consequence, absolute Co $2p_{3/2}$ intensity is overestimated by ca. 15% [11,12].

Before carrying the CO adsorption, the reduced samples were preformed as pellets with the density 15–20 mg/cm^2. Then the plates were placed into a quartz cell, treated in vacuum at 450°C for 30 min, reduced with hydrogen at 450°C for 30 min and, finally, treated in vacuum once again at 450°C for 30 min.

The in situ FTIR spectra of the adsorbed CO molecules were recorded by means of a SHIMADZU-8300 FTIR spectrometer with resolution of 4 cm^{-1} and the scans number 50. The spectra of the studied samples before the CO adsorption, as well as those of the gaseous phase after the experiments were subtracted from the total FTIR spectra.

3. Results

Both series (CA and PZA) of the samples have been characterized by IR spectroscopy, while only CA series of the samples have been used for XPS study. Rejection from XPS study of the PZA samples is explained by volatility of zinc in high vacuum conditions of the electron spectrometer. Enhanced background pressure of Zn remains for a long time that is very hazardous for further XPS experiments. Nevertheless, XPS data for the CA samples can be propagated to the PZA ones, since both series exhibit similar tendencies in variation of their catalytic properties depending on pre-treatment conditions in the CO hydrogenation.

The characterization of the samples by the STA, TPR, FTIR spectroscopy, XRD, as well as their catalytic properties in the CO hydrogenation were reported earlier in [9] (samples CA-II and P/ZA).

3.1. X-Ray photoelectron spectroscopy

Elemental composition of surface and subsurface layers (depth of XPS analysis makes up tens of angstrom) of the initial Co-Al sample can be observed from survey XPS spectrum shown in Fig. 1. Except for the lines of the main elements: cobalt, aluminum and oxygen, carbon is detected from this spectrum.

Table 1 presents atomic fractions (%) of C, Al, O, Co and their atomic ratios determined from the intensities of the corresponding core level XPS lines (C 1s, Al 2p, O 1s and Co 2p) corrected on atomic sensitivity factors (ASF) [10]. One can see that the content of carbon is rather considerable and has a maximum for the inital sample (26%) decreasing under sample treatment (to 11.2% in the CA-HT one). As a rule, impurities of carbon have a double origin. It can be introduced both on stages of sample preparation and as a result of hydrocarbon adsorption during the sample evacuation inside the electron spectrometer. The C 1s core level spectra shown in Fig. 2 confirm this suggestion. Indeed, the spectrum of the original CA-U sample exhibits two features with different intensities (see Fig. 2).

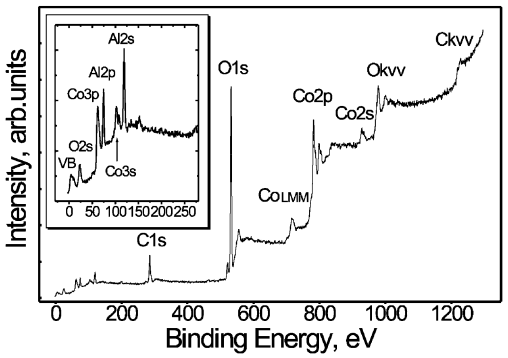

Fig. 1. XPS survey spectrum of the sample CA-U.

The most intense line at 284.8 eV (FWHM = 2.4 eV) is associated with an elementary carbon intercalated into the bulk of catalysts and/or with hydrocarbon residues adsorbed on the surface. The second weak feature at 289.6 eV is assigned to the carbon atoms bonded with several oxygen atoms (e.g. carboxyl or carbonate groups). Full disappearance of the latter signal is observed after heating the sample at 650°C (see Table 1).

The assignment of Al 2p and O 1s core level spectra presented in Figs. 3A and 4A, respectively, are much

Table 1
X-ray photoelectron spectroscopy surface elemental concentrations (at.%) as well as the relative surface concentration of the elements

Sample	C	O	Al	Co	Co/Al	C/Al	C[a]/Al	(Al + Co)/O
CA-U	26.0	52.8	7.4	13.5	1.85	3.51	0.41	0.40
CA-C	16.3	52.1	11.4	20.2	1.79	1.43	0.08	0.61
CA-LT	12.7	53.5	13.3	20.5	1.54	0.95	0.05	0.63
CA-HT	11.2	60.1	19.8	8.9	0.45	0.57	0.00	0.48

[a] Only for CO_3^{2-} species.

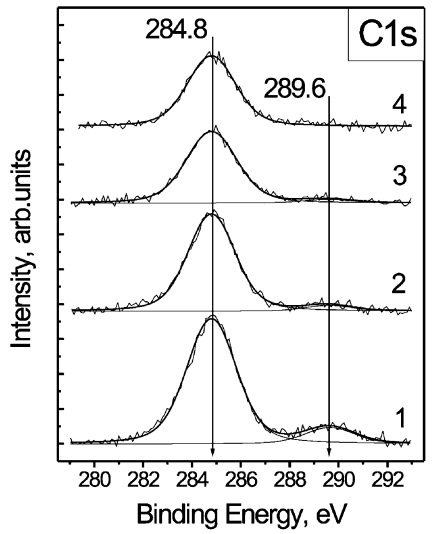

Fig. 2. XPS C 1s spectra of the studied samples: (1) CA-U, (2) CA-C, (3) CA-LT, (4) CA-HT.

less evident. Indeed, these spectra are broad and featureless that makes it ambiguous to decompose them on separate components. To tackle this problem and to follow the evaluation of Al and O chemical states during the catalyst activation we have prepared difference spectra (Figs. 3B and 4B).

One can see that in full agreement with quantitative data (Table 1) only positive part is registered in the Al 2p difference spectra indicating a constant increase in surface concentration of Al. This gain of aluminum content is accompanied by the variation of Al 2p binding energies, which decrease at calcination and increase when the catalyst is underwent by reduction. This statement is based on the appearance of two additional components at 74.0 (Fig. 3B, curve 2–1) and 75.1 eV (Fig. 3B, curves 3–2 and 4–3), respectively. It should also be noted that the feature at 75.1 eV appearing as result of hydrogen treatment does not change the position with temperature, but increase its intensity only. In spite of 1 eV differences in binding energies, all the observed features can be assigned to Al^{3+} cations bonded with oxygen [13,14], with BE variation being explained by the changes in aluminum coordination and/or in defectiveness of the structure.

Similar picture is observed for the O 1s difference spectra (Fig. 4B). Calcination in air gives rise to new feature at 530.4 eV that is accompanied by the removal of a feature at 532.5 eV. This behavior is in good agreement with expected dehydration of the

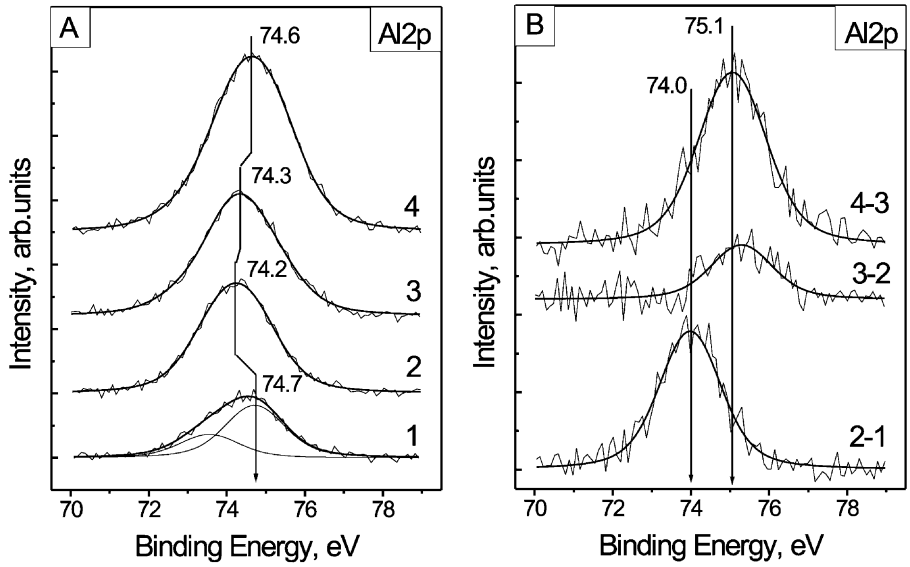

Fig. 3. (A) Al 2p region of the X-ray photoelectron spectra of the samples CA: (1) CA-U, (2) CA-C, (3) CA-LT, (4) CA-HT; (B) the differential spectra.

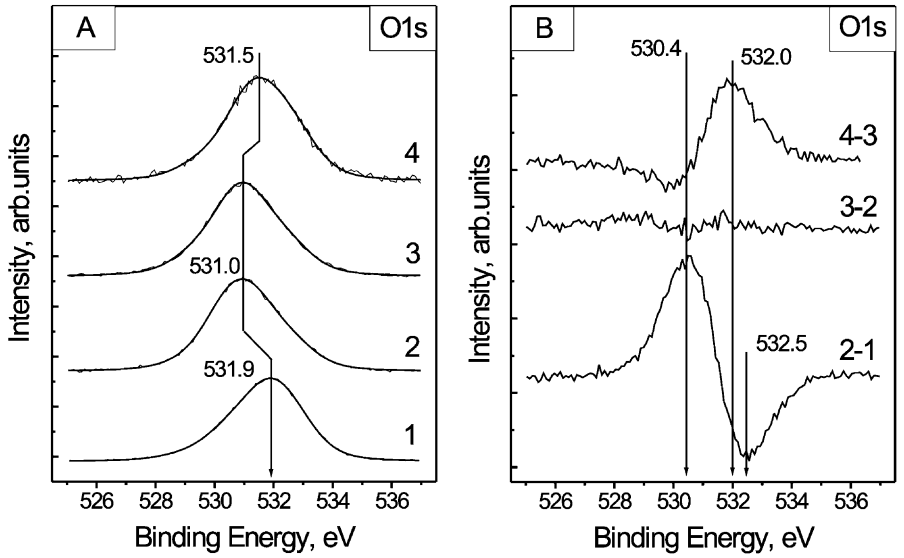

Fig. 4. (A) XPS O 1s spectra of the studied samples: (1) CA-U, (2) CA-C, (3) CA-LT, (4) CA-HT; (B) difference spectra.

surface of the initial sample. Indeed, according to literature data aluminum hydroxides are characterized by O 1s binding energies of 531–532.5 eV and oxygen in spinel structure — 530.4 eV [13–16]. Subsequent reduction of the catalyst causes development of new component with BE = 531.9 eV in addition of the main line at 531.0 eV. The possible explanation of the observed spectra evolution will be discussed later.

The Co 2p core level spectrum is characterized by two components appearing due to spin-orbital splitting — Co $2p_{3/2}$ and Co $2p_{1/2}$, and shake-up satellites. On one hand, these features complicate the analysis of the spectrum shape, but, on the other hand, provide additional arguments to assign the Co 2p features observed in this complex spectrum. Indeed, the intensity ratio and BE separation of the satellite signals from the Co $2p_{3/2}$/Co $2p_{1/2}$ photolines, as well as spin orbital splitting, are dependent on the chemical state of cobalt. The high spin Co^{2+} compounds such as CoO, $Co(OH)_2$ and $CoAl_2O_4$ exhibit strong satellite lines which are located at about 5–6 eV above the photo line [15,18]. Contrary to that, very weak satellite, to be shifted about 10–11 eV to higher binding energies from the main peak, is characteristic of the low spin Co^{3+} compounds (Co_3O_4, CoOOH) [18]. The spectrum of metallic cobalt does not contain shake-up satellite structure at all. The exact values of the Co $2p_{3/2}$ binding energy and BE separation between the components of Co 2p doublet can be found in Table 2. These literature data have been used for comprehensive analysis of the Co 2p spectra of our samples presented in Fig. 5. To extract the values mentioned above, we deconvoluted the Co 2p spectra on separate component and prepared difference spectra. The corresponding values are collected in Table 3.

One can see that the initial Co-Al sample is characterized by a Co $2p_{3/2}$ feature at 781.5 eV (FWHM = 3.6 eV) and a relatively intense shake-up satellite peak at 786.2 eV. Spin-orbital splitting between the Co $2p_{3/2}$ and Co $2p_{1/2}$ peaks is 15.9 eV. These observations allow us to describe the chemical state of cobalt as Co^{2+} and to exclude practically the existence of Co^{3+} ions.

The calcination of the initial sample broadens the Co $2p_{3/2}$ spectrum with low binding energy side that results in small shift of the doublet lines to 781.2 eV (Table 3). The corresponding difference spectrum (Fig. 5B, curve 2–1) shows that the appearance of additional component with BE = 780.9 eV with high value of spin-orbital splitting (15.8 eV) is responsible for such behavior of the spectra. It should be also noted that the appearance of new Co $2p_{3/2}$ feature is not accompanied by the variation of relative intensity of the satellite peak. All these facts allow us to assign

Table 2
XPS data of cobalt-containing reference materials[a,b]

Co^0		CoO		$CoAl_2O_4$		$Co(OH)_2$		Co_3O_4		Reference
BE Co $2p_{3/2}$	Spin-orbit coupling	BE Co $2p_{3/2}$	Spin-orbit coupling	BE Co $2p_{3/2}$	Spin-orbit coupling	BE Co $2p_{3/2}$	Spin-orbit coupling	BE Co $2p_{3/2}$	Spin-orbit coupling	
		780.7						780.1	15.0	[12]
777.7		779.7		780.3		780.7		779.6[c]		[15]
778.0		780.3				781.1		779.5		[16][d]
778.1	15.1	780.1	15.5	781.7	15.5	780.9	16.0	780.5	15.0	[17]
		781.0	15.9	782.0	15.3			779.6	15.2	[18]
777.7		781.7						779.8		[19]
777.9				781.8				780.2		[20]
777.5				781.8				780.6		[21]

[a] All values are presented in eV.
[b] All data are referenced to the C 1s = 284.8 eV BE.
[c] For Co_2O_3.
[d] These data are referenced to the Au $4f_{7/2}$ = 84.0 eV BE.

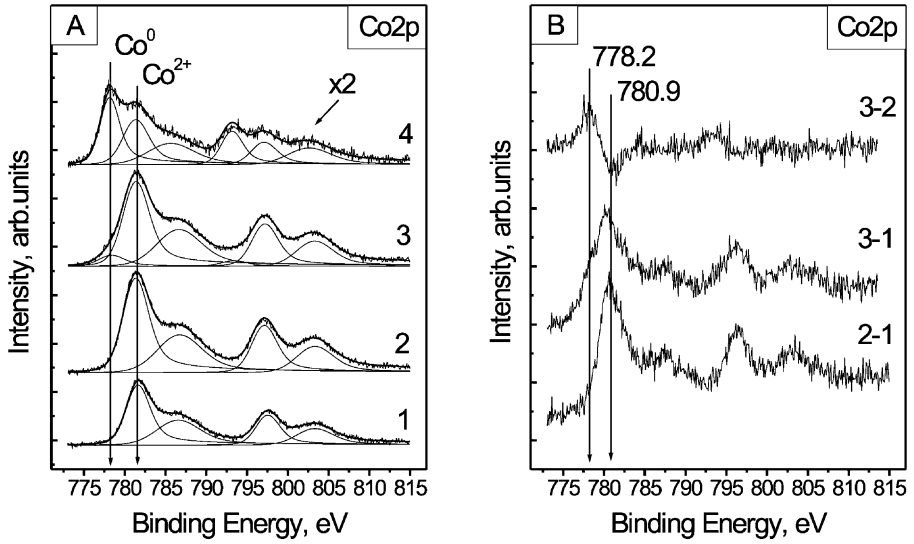

Fig. 5. (A) XPS Co 2p spectra of the studied samples: (1) CA-U, (2) CA-C, (3) CA-LT, (4) CA-HT; (B) difference spectra.

Table 3
The results of XPS Co 2p spectra decomposition: binding energies (eV), magnitudes of the spin-orbit splitting (eV), as well as the calculated surface atomic ratio of Co^0 species to total cobalt content

Sample	Co $2p_{3/2}$ (Co^0)	Spin-orbit coupling (Co^0)	Co $2p_{3/2}$ (Co^{2+})	Spin-orbit coupling (Co^{2+})	Co^0/Co
CA-U	–	–	781.5	15.9	0
CA-C	–	–	781.2	15.8	0
CA-LT	778.2	15.0	781.2	15.8	0.07
CA-HT	778.0	15.0	781.2	15.7	0.38

it mostly to Co^{2+} and, as consequence, to suggest the formation of cobalt-containing oxide phase during the calcination.

Reduction of the calcined sample by hydrogen gives rise to one more Co $2p_{3/2}$ feature at 778.1 ± 0.1 eV which is clearly seen both in difference spectrum and after deconvolution of integral spectra. This feature can be unambiguously assigned to metallic cobalt, its concentration in the studied samples being enhanced at raising the reduction temperature. These conclusions are in good agreement with our earlier data of X-ray diffraction (XRD) and transmission electron microscopy (TEM), which detected the presence of cobalt metallic particles with size about 50–100 Å in CA-LT and CA-HT samples [9]. The deconvolution of the Co 2p spectra for the reduced samples allows us to determine the relative amount of Co^{2+} and Co^0 species (see Table 3).

3.2. The interaction of CO with the catalysts under the study

Fig. 6 presents the FTIR spectra of CO molecules adsorbed over Zn-Co-Al samples PZA-C, PZA-LT and PZA-HT at 77 K. The FTIR spectra of CO adsorbed over zinc-free samples CA at 77 K are very similar to those in Fig. 6.

The spectra of CO molecules adsorbed over the calcined sample PZA-C contain bands at ca. 2156 and 2191 cm^{-1}, which lie at higher frequencies than that of gaseous CO (2143 cm^{-1}) and, therefore, should be attributed to CO–Me^{n+} species. According to the previous studies [22], the most intense band at 2154–2156 cm^{-1} should be attributed to CO–Co^{2+} species. The higher frequency band has maximum near 2191 cm^{-1} at lowest coverage and shifts to near 2180 cm^{-1} at a higher coverage. Earlier, a band at 2190 cm^{-1} was reported for the CO molecules adsorbed over Co_3O_4 [23,24]. On the other hand, the similar absorption band at 2185–2195 cm^{-1} was assigned to the CO molecule bonded to the octahedrally coordinated Al^{3+} cations of high Lewis acidity [22]. A week band at 2060 cm^{-1} may be attributed to the CO molecules adsorbed at Co^0 species forming due to a partial reduction of the Co^{2+} surface species during their vacuum treatment, which preceded the measurements in CO. The presence of the low-frequency bands in the spectra of CO adsorbed over the Co oxides was observed earlier (e.g. for CoO/MgO [25,26] and for Co_3O_4 [24]).

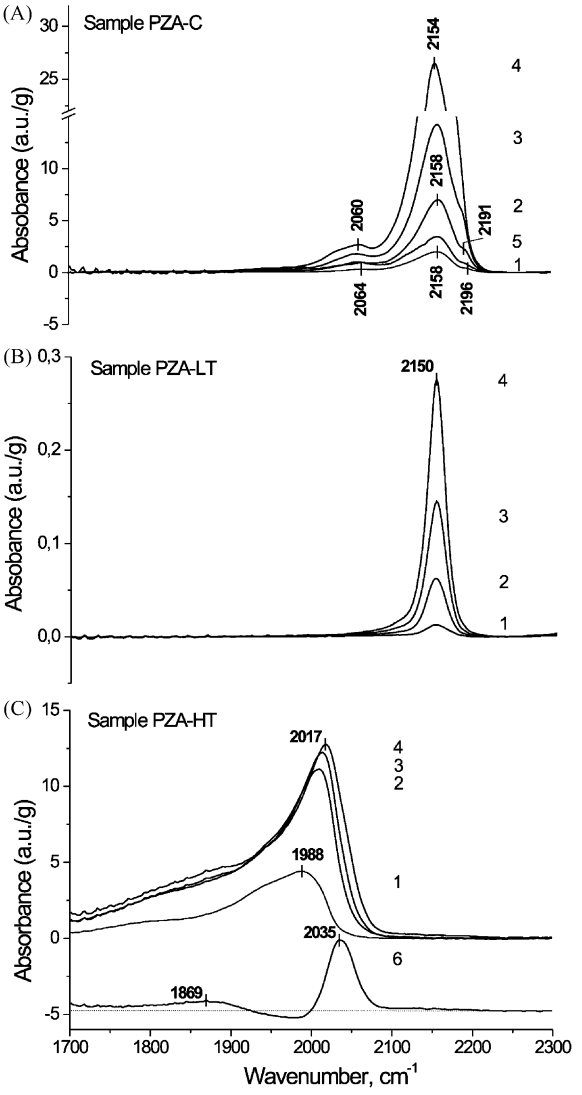

Fig. 6. FTIR spectra of the CO adsorbed on the samples PZA: (A) the calcined sample, PZA-C; (B) the reduced at 480°C sample, PZA-LT; (C) the reduced at 650°C sample, PZA-HT; (1) $T = 77$ K, $P_{CO} = 0.02$ Torr; (2) $T = 77$ K, $P_{CO} = 0.08$ Torr; (3) $T = 77$ K, $P_{CO} = 0.18$ Torr; (4) $T = 77$ K, $P_{CO} = 10$ Torr; (5) $T = 298$ K, $P = 10$ Torr; (6) the difference between spectra (4) and (2).

The spectra of CO adsorbed at 77 K over sample PZA-HT (reduced at 650°C) do not contain the bands with the wavenumber above 2100 cm^{-1}. This fact indicates the absence of any CO–Co^{n+} species at

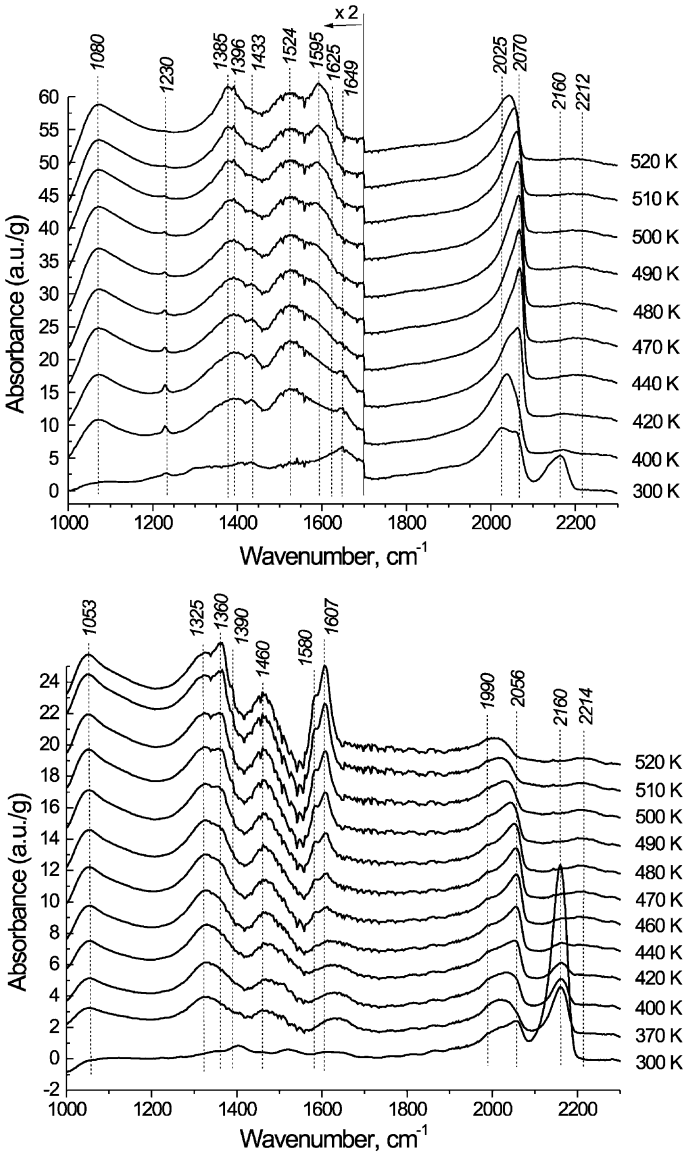

Fig. 7. In situ FTIR spectra of CO adsorbed on samples CA: the reduced at 650°C sample, CA-HT (the upper graph); and the reduced at 480°C sample, CA-LT (the lower graph). The spectrum of water vapor was subtracted from the experimental data. $P_{CO} = 10$ Torr.

the surface of the sample. The bands at 1870, 1990, and 2035 cm^{-1} may be attributed to the bridged CO [27,28], terminal CO [2,27,29,30] and carbonyl $Co(CO)_X$ ($X > 1$) [31] species, correspondingly. The formation of multi-carbonyl species takes place only at a relatively high coverage.

Of a special interest are the spectra of CO adsorbed at 77 K over sample PZA-LT (reduced at 480°C). This sample does not adsorb CO at 77 K, but a tiny quantity of weakly (probably — physically) adsorbed species is detected by FTIR (the band at 2150 cm^{-1} is symmetric and very close to that of gaseous CO).

Fig. 7 presents the IR spectra of CO over the CA-LT and CA-HT sample surfaces at elevated temperatures and CO pressure of 10 Torr. Carbonyl, carboxyl, carbonate and formate species are evidently formed

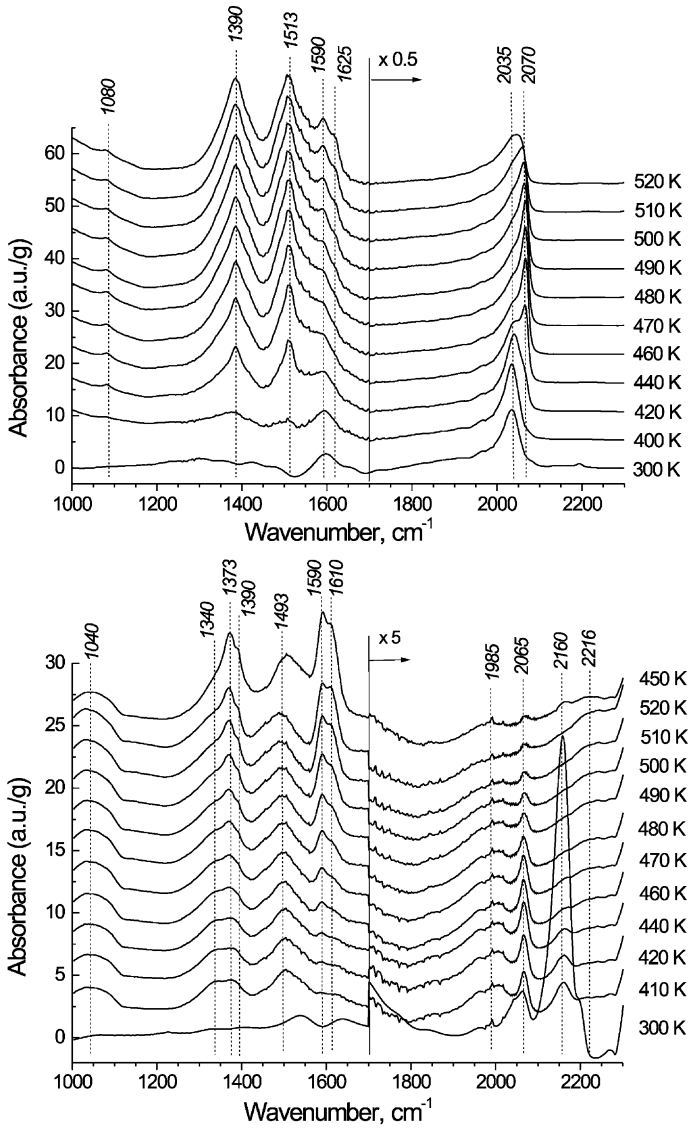

Fig. 8. In situ FTIR spectra of CO adsorbed on samples PZA: the reduced at 650°C sample, PZA-HT (the upper graph); and the reduced at 480°C sample, PZA-LT (the lower graph). The spectrum of water vapor was subtracted from the experimental data. $P_{CO} = 10$ Torr.

during the adsorption. The analogous spectra for PZA samples are shown in Fig. 8. The characteristic wavenumbers and the band assignments are given in Table 4.

At the elevated temperatures, no adsorption which can be attributed to the CO–Co^{3+} species was detected. The adsorption band at ca. 2160 cm^{-1} vanishes rapidly at raising the temperature. This is typical for the CO species adsorbed on Co^{2+} [24]. The band at 2214 cm^{-1} appears at the temperatures above 100°C and most likely should be assigned to the CO–Al^{3+} species. Usually, the bands at 2190–2230 cm^{-1} are registered for the CO–Al^{3+} species.

The carbonyl species (bands at 1980–2070 cm^{-1}) are present in all studied samples. However, the catalyst activation temperature affected the amount of

Table 4
The characteristic wavenumbers (cm^{-1}) and the assignments of the FTIR absorption bands of the CO molecules adsorbed on the samples under the study

Assignment		CA-HT	CA-LT	PZA-HT	PZA-LT
Unidentate carbonate	ν_{C-O}	1080	1053	1080	1040
	ν_sCOO	1390	1325	1391	1340
	ν_{as}COO	1524	1462	1514	1493
Carboxylate	ν_sCOO	1390	1390	1390	1390
	ν_{as}COO	1595	1580	1590	1590
Formate	ν_sCOO	1396	1360	1390	1373
	ν_{as}COO	1625	1607	1626	1610
Bicarbonate		1230	Traces at ca. 1230		
		1433	Traces at ca. 1440		
		1649	Traces at ca. 1650		
Carbonyl	CO–Co^0 terminal "non-tilted"	2070	2056	2070	2065
	CO–Co^0 terminal "tilted"	2025	1990	2035	1985
	CO–Co^{2+}	2164	2160	–	2160
	CO–Al^{3+}	2212	2214	–	2216

these species dramatically. For the CA-HT sample, the CO–Co^0 absorption bands are at least three times more intensive than those for the sample CA-LT. Moreover, for the PZA samples the difference in the intensities achieves the factor of 15. Analysis of the band shape and its evolution at the temperature increase evidences that mostly two types of the CO–Co^0 species are present at the sample surface (the absorption bands at ca. 2050–2070 and 1980–2040 cm^{-1}). Following the earlier studies [2,23,32], we attribute these to the terminal CO species, which are adsorbed at the metallic Co particles. Actually, according to the literature data bridged $\left(\begin{matrix}Co\\Co\end{matrix}>CO\right)$ species should absorb IR radiation at lower energies range (1800–1900 cm^{-1}). Thus, both bands (at 1980–2040 and 2050–2070 cm^{-1}) should be attributed to the terminal carbonyl.

We failed to find the exact explanation for the observed difference in the bands maxima positions, despite the similar inhomogeneity of the carbonyl absorption band for CO adsorbed on Co^0 was observed earlier in literature. Apparently, the absorption at 2050–2070 cm^{-1} is related to the CO group, which is perpendicular to the surface. The lower C–O band strength for the other type of carbonyl species (absorption at ca. 1980–2040 cm^{-1}) could be an indication to the secondary interaction of the CO species with a neighboring cobalt atom (adatom), which should cause the lateral tilt of the CO group. It should be noted, that the existence of the lateral tilt of the absorbed CO may be accompanied by the significant stabilization of CO adsorption by means of 4σ-, 5σ- and 1π-donation toward an metal adatom [33]. At the same time, it results in significant lengthening of the C–O bond (from 1.16 to 1.19 Å for the 65° tilt in the case of CO adsorbed on Fe [34]). Structural works shows that CO is bound perpendicularly to Fe(1 1 0) and strongly tilted relative to surface normal at Fe(1 0 0) (see, e.g. [35]). Basing on these data we suppose, that the observed carbonyl species may differ by their lateral tilt (ca. 2050–2070 cm^{-1} for "non-tilted" or "perpendicular" CO species, and ca. 1980–2040 cm^{-1} for the "tilted" ones). Apparently, the nature and specific features of "tilted" carbonyls over cobalt surface needs further investigation by physical methods.

At low temperatures, bicarbonates and monodentate carbonates are detected in the region $<1700\,cm^{-1}$. The temperature increase resulted in the rapid removal of bicarbonates. The amount of the monodentate carbonate species increases monotonously with the temperature in the studied temperature range. The concentrations of these species is higher in the samples reduced at 650°C, than in those reduced at 480°C. The bands at 1300–1400 cm^{-1} could be partly attributed to formate species located on Al^{3+} cations of the support,

which form by interaction of CO with the Al–OH surface groups. The weak band at ca. 1630 cm^{-1}, which is well resolved for the sample CA-LT is plausibly related to Al^{3+}-formates as well.

The temperature increase up to 100–150°C leads to the appearance of the bands which we attribute to the carboxyl (1390 cm^{-1}) and formate (1360, 1396, 1607 and 1625 cm^{-1}) groups. It is noteworthy that despite the band at 1625 cm^{-1} (1607 cm^{-1} for the LT samples) may be attributed to water formation, the similarity in behavior of this band to that of the band at 1396 cm^{-1} (1360 cm^{-1} for the LT samples) forces us to attribute both bands to the formate species. Their concentration increases with the temperature and seems to be of the same order of magnitude for the LT and HT samples.

It follows from Figs. 7 and 8 and Table 4, that the positions of the band maxima are coincident for the two HT samples (CA-HT and PZA-HT) reduced at 650°C. However, they are dramatically different for the LT samples reduced at 480°C. An obvious shift to the range of lower frequencies (as compared to the HT samples) was observed for the bands related to carbonyl species (2070 and 2025 cm^{-1} for the CA-HT sample to 2056 and 1990 cm^{-1} for the CA-LT sample), as well as for the formate species (1625 and 1396 to 1607 and 1360 cm^{-1}) and the monodentate carbonates (1080, 1390, 1524–1053, 1325 and 1462 cm^{-1}). This shift will be further denoted as a "red shift". The positions of the absorption maxima of the CO–Me^{n+} species and of carboxyls are the same for all four samples studied.

4. Discussion

4.1. The evolution of the Co-Al sample structure according to XPS

The above reported XPS data are in a good agreement with our earlier conclusion [9], that the uncalcined catalyst appears to be Co-Al hydroxycarbonate with the hydrotalcite-like structure, $CoAl(OH)_x(CO_3)_y \cdot nH_2O$. One can notice from Table 1, that the surface ratio of the Co concentration to that of Al in the uncalcined sample is much higher, than that for the bulk stoichiometry of this sample. In other words, the segregation of cobalt from the catalyst bulk to the surface takes place, resulting in an enrichment of the surface brucite-like layer of hydrotalcite structure by divalent cations (Co^{2+}).

The calcination of the sample at 500°C in the argon flow causes the shift of Co 2p photoemission to lower binding energies (ca. 781.2 eV), a decrease of the spin-orbital splitting value and a sharp decrease of the CO_3^{2-} groups content (see the data for sample CA-C). These observations are consistent with decomposition of the initial hydrotalcite-like structure and formation of a $Co^{2+}Al_2O_{4-y-z}(OH)_{2y}(CO_3^{2-})_z$ oxide. This is approved by appearance of new features in the Al 2p and O 1s spectra at 74.0 and 530.4 eV, correspondingly, (Figs. 3 and 4, curves 2–1), which are specific for the $CoAl_2O_4$ spinel structure [15]. Note that the disappearance of the O 1s signal at 532.6 eV is ascribed to the removal of crystal water from the sample.

The reduction of the sample leads to the further removal of the carbonate groups (samples CA-C and CA-LT) and, finally, their total vanishing during the reduction at 650°C (sample CA-HT). The intensity variation of the feature at 289.6 eV correlates well with the IR spectroscopy and STA data of our earlier study [9]: the partial removal of CO_3^{2-} groups of the initial hydrotalcite structure was observed during the sample calcination and its reduction at 480°C, while the reduction at 650°C led to their total removal. The monotonous decrease of the oxygen surface concentration in the row CA-U > CA-C > CA-LT can be explained by the removal of the hydroxyl and carbonate groups from the catalyst structure. Thus, the XPS data give an additional support for the earlier proposition about the anionic modification of the spinel-like phase of the Co-Al oxide.

The increase of both the aluminum surface atomic concentration and the Al/Co ratio are probably due to the formation of alumina agglomerates during the calcination of the studied samples (see Table 1). The increased photoemission at 75.1 eV, which is simultaneous with the reduction of cobalt to Co^0, may be ascribed to some Al^{3+} species at the metal–support interface. Indeed, the maxima in the difference Al 2p spectra at 75.1–75.5 and at 531.9 eV in O 1s ones (Figs. 3 and 4; curves 3–2) are typical of amorphous clusters of Al_2O_3 or thin alumina films located on surface of metallic particle [8,36].

Table 5 presents (i) the surface concentration of Co^0 in respect to the total surface concentration of the

Table 5
The summary of the data on the Co content in the samples under the study, as well as the data on the specific activity of the samples in CO hydrogenation rection

	CA-HT	CA-LT	PZA-HT	PZA-LT
Ratio Co^0/Co (%)				
Bulk Co^0 (from O_2 titration at 450°C [9])	63	34	108	76
"Accessible" Co^0 (from O_2 titration at 200–250°C [9])	51	19	65	61
Surface Co^0 (from XPS)	38	7	–	–
The intensity of the band at 2050–2070 cm^{-1}, a.u./g cat (an estimation for the amount of CO–Co^0 species)	17	3	37	0.8
The rate of CO hydrogenation, $T = 503$ K, $P = 1$ bar, $H_2/CO = 2$ [9], μmol/g cat/h	1880	80	650	20

cobalt species, as it was determined from the XP spectra, (ii) the data on the bulk content of Co^0 determined by the temperature programmed oxidation [9], (iii) the concentration of the surface carbonyl species during the CO adsorption studies, and (iv) the experimental data on the sample activity in the CO hydrogenation [9]. Note that according to the data of [9], the oxidation of the Co^0 particles proceeds in two steps: <250 and at 250–450°C. The latter oxidation was attributed to some "non-accessible" Co^0 particles, i.e. those encapsulated into the Co-Al oxide support. The data of Table 5 evidence, that the sample's activity correlates both with the surface concentration of the carbonyl species and the surface concentration of Co^0. However, the correlation of these values with the data on the bulk concentration of Co^0 is much more poor. For the samples CA-LT and PZA-LT, the bulk concentrations of the Co^0 species are much higher than it follows from the data on the surface species. One can note also, that the activity of the catalyst CA-LT in the CO hydrogenation is still much less, than it could be expected from the FTIR data. The relation of the earlier reported catalytic properties to the data under consideration will be discussed below.

The above mentioned mismatch of the presented data to the data on the bulk titration by O_2 may be explained by supposing, that the Co^0 particles are partially covered by an aluminum oxide phase, which diminishes the Co^0 surface but does not prevent the whole Co^0 particle from oxidation during the O_2 titration procedure. Turning back to the speculation on the Al 2p photoemission spectra, one can note that the latter supposition accords with the abnormally high Al 2p binding energy 75.1 eV.

4.2. The red shifts of the IR absorption bands

4.2.1. The red shifts of the carbonyl species IR bands

The red shifts of the IR bands from the carbonyl species on the surface of the CA-LT and PZA-LT samples (Figs. 7 and 8) are equal to 5–15 cm^{-1} for the "non-tilted" CO species and 25–40 cm^{-1} for the "tilted" CO species. These shifts cannot be attributed to any artifact. Thus, one should suppose that a weaker C–O band is the sequence of the electron properties of metallic particles, which comprise the LT samples. As it follows from the Blyholder model, the CO chemisorption can, in the first approximation, be described as a sum of two contributions: firstly, the metallic particle accepts electron from the 5σ bonding molecular orbital of CO; secondly, the back-donation of electron to the $2\pi^*$ antibonding molecular orbital of CO [33,37]. Despite CO is considered traditionally as a pronounced π-acceptor, the impact of the σ-donation is significant and the CO adsorption can not be described by one of these two interactions alone [38]. The 5σ-donation should be increased, if the metal has an effective positive charge. The impact of the π back-donation should become more significant, if the effective charge is negative. One can discriminate between these two plausible reasons via comparing the values of IR band shifts for "non-tilted" terminal and "tilted" terminal carbonyls. It is well known, that the impact of the 5σ-donation is more pronounced for bridged species (due to a better overlap of the 5σ orbital and the partially filled d(*xy*) band of Co), while terminal CO acts mostly as a π-acceptor. It could be supposed that the impact of the 5σ-donation is more expressed for "tilted" CO, rather than for

the "non-tilted" species. It is evident from Figs. 7 and 8 and from Table 4 that the IR band position of the "tilted" species is twice or three times more shifted, than that of the non-tilted CO species. Therefore, the red shift of the IR bands indicates a more strong acceptance of the 5σ electron of CO by the metal, i.e. the positive charging of Co particles. Thus, the Co particle should be ascribed as a Co^0 particle with a more strong electron-acceptor capability or as $Co^{\delta+}$.

Similar assignment is not unusual and can be found in literature. Earlier, Lapidus et al. [2], who have measured the IR spectra of the CO molecules adsorbed on the surface of the impregnated Co/Al_2O_3 samples, assigned the absorption at 2050 cm^{-1} to the CO molecules adsorbed on the surface of the Co^0 particles with the "less marked electron-donor capability" or the "$Co^{\delta+}$" particles. Kadinov et al. [39], attributed the similar absorption for the Co/Al_2O_3 catalysts reduced at 723 K to the $Co^{\delta+}$–CO species.

A distinguishing feature of the present data is that the absorption band at 2056 cm^{-1} is a dominant absorption band of the CO molecules adsorbed on the CA-LT catalyst. The bands are obviously shifted to the region of lower frequencies, when compared to the HT samples.

The proposed above effective positive charging of the metallic particle could be a sequence of the formation of a two-dimensional molecular-size clusters of an aluminum oxide at the surface of the metallic Co particle, that was already discussed above. Then, taking into account the small size of a cluster, one can expect that its stoichiometry is $Al_{2x}O_{3x+y}$, where y is some positive number. Then, the $Al_{2x}O_{3x+y}$ cluster acts as an electronegative ligand for the $Co_z{}^0$ cluster forming a $(Co_z)^{2y+}(Al_{2x}O_{3x+y})^{2y-}$ complex. Note that the experimental data force us to conclude, that the OH^- and/or $CO_3{}^{2-}$ groups should be present in the support for the stabilization of the above nano-scale oxide cluster: the most important difference of the LT samples from the HT ones is the anionic composition of the oxide support (see [9]). Actually, at the presence of OH^- groups the formation of the $(Co_z)^{2y-w}(Al_{2x}O_{3x+y-w}OH_w)^{w-2y}$ complex may be expected to be more thermodynamically favorable, than at their absence, since the OH^- — promoted spinel-like structure is more "flexible" to its distorting than the ideal spinel structure.

In [32], the similar red shift of the carbonyl IR bands was reported for a Na^+-promoted silica-supported nickel catalyst. The DRIFT spectra of the unpromoted sample contained the bands at 2067 and 1920 cm^{-1} which are shifted to 2057 and 1780 cm^{-1} for the sodium containing sample. The catalytic properties of the $Na\text{-}Co/Al_2O_3$ and $Na\text{-}Ni/SiO_2$ catalysts in CO hydrogenation were found there to be very close to those for the LT samples under discussion. One should mark a similarity of the effect of Na^+ [32] and H^+ [9] on the performance of the Co and Ni catalysts in the FTS. This may be an indication of an alkali metal cation (or proton) promotion in a the stabilization of the nano-scale Al-oxide cluster at the metallic surface resulting in the formation of the above discussed complex.

4.2.2. The red shifts of the IR bands of the carbonate and formate species

The similar red shifts have been observed also for the monodentate carbonates as well as for the formate species which form on the catalyst surface during the CO adsorption. This leads us to suggestion that both of these species are adsorbed on the metal. For the formate species, the simultaneous growth of the absorption bands at ca. 1396 and 1625 cm^{-1} (or 1360 and 1607 cm^{-1} for *-LT samples) is accompanied by a diminishing the intensity of the band at ca. 2050–2070 cm^{-1}. This indicates, probably, that the formate species are a result of an interaction of the terminal CO species with the water vapor at the metal-oxide interface.

The stabilization of the monodentate carbonates at the metal surface during the CO adsorption seems to be somewhat amazing. However, the correlation of their surface concentration with the concentration of the CO–Co^0 species and the apparent red shift of the corresponding absorption bands for *-LT samples forces us to insist upon this attribution. Note that CO molecules do not disproportionate at temperature as low as 500 K. The CA-HT and PZA-HT samples exhibited activity in the carbon filaments formation only at temperatures above 550 K, while CA-LT and PZA-LT — only above 650–700 K [40]. The phenomenon may be explained in terms of the suggestion about the formation of small Al^{3+} oxide clusters at the metallic surface. In this case, the carbonate species may form at the expense

of the interfacial oxygen atoms of the oxide cluster.

The carboxyl moieties as well as the $CO–Co^{2+}$ and $CO–Al^{3+}$ species are not sensitive to the sample reduction temperature. Therefore, these species seem to be located on the surface of the oxide support, rather than on the reduced metal.

4.3. The relation of the present data to earlier data on the catalytic properties

The reported catalytic properties of some Co-Al catalysts differ a lot from those of the "normal" Co^0 in at least four reactions: $H_2–D_2$ exchange [8], CO oxidation [7], CO hydrogenation [9,32] and ethylene hydrogenation [8,41]. The Co-Al catalysts have been found to be substantially inactive in all these reactions at the temperatures <200–300°C. The experimental data of the current paper could give a key for understanding of the nature of these phenomena.

Actually, all the catalysts, which have "abnormal" catalytic properties, were also reported to contain simultaneously a Co^0 phase and amorphous γ-Al_2O_3 phase or Al-containing oxide. "Abnormal" Co-Al catalyst studied in [7] was prepared by a technique, which provided chemical interaction of Co and Al in the presence of the OH^- groups, i.e. this sample properties can be expected to be close to those of the CA-LT and PZA-LT samples. Other authors suggested that the Co^0 particles were decorated by an Al_2O_3 oxide [8]. This suggestion was based on the experimental XPS data. Thus, one may expect, that the phenomena observed in the quoted papers and in the present study are of the same nature.

4.3.1. Conversion of CO over SMSI Co-Al catalysts

A low activity of the "abnormal" (further denoted as "SMSI") Co-Al catalysts in the CO oxidation and CO hydrogenation correlates with the IR data which indicate that no adsorption of CO occurs at the PZA-LT sample at temperatures <25°C. The "SMSI" Co-Al catalysts are not able to activate CO at low temperatures. Therefore, at low temperatures (77 K), the resulting interaction of the CO molecule and the SMSI $Co^{\delta+}$ is repulsive. At elevated temperatures, the CO adsorption occurs, however, the shifted positions of the CO vibration adsorption bands indicate a stronger impact of the σ-donation in the interaction of the CO molecule and Co particle as the result of the effective positive charging of the Co particle. The IR data indicate an enhanced stabilization of the CO molecule over SMSI Co^0 relatively to the "normal" Co^0.

Another reason of the Co inertness is diminishing of the metallic surface due to covering the metallic particle by nano-scale aluminum oxide clusters. According to our data, only 10–40% of the metallic surface is available to the gas molecules.

Despite the above peculiarities of SMSI, Co may result in its lower activity in relation to the CO conversion reactions (CO hydrogenation and CO oxidation), it hardly can explain the observed lack of its activity at the elevated temperatures by a factor >30 [7,9]. Thus, one should conclude, that the SMSI Co-Al catalysts are not able to activate H_2 and O_2 molecules at low temperatures. Actually, this supposition is in the agreement with the data of [8], where an inertness of the Co^0-Al_2O_3-Al^0 catalyst in the reaction of $H_2–D_2$ exchange was shown. It is also consistent with the data of [9], where the "SMSI" Co was shown to oxidize resulting in formation of Co oxides only at the elevated temperatures (>200–250°C).

The nature of H_2 and O_2 interaction with SMSI $Co^{\delta+}$ is not clear and needs a further investigation (including theoretical quantum chemical studies).

4.3.2. Conversion of C_2H_4 over SMSI Co-Al catalysts

The data of [9,32] evidence that the SMSI Co-Al catalysts promoted by either OH^- (i.e. H^+), or Na^+ have an extremely high selectivity towards olefins (particularly — to ethylene) formation at CO hydrogenation. This indicates unambiguously, that ethylene does not re-adsorb on SMSI cobalt. The data of [8,41] give further proves that SMSI cobalt is not able to activate ethylene at temperatures <150–200°C. This is consistent to the above made conclusions on the nature of the CO interaction with SMSI $Co^{\delta+}$. Actually, the electron structure of ethylene is similar to that of CO. However, ethylene is a pronounced π-acceptor. Therefore, the effective positive charging of $Co^{\delta+}$ could make the interaction with C_2H_4 be repulsive.

5. Conclusions

1. The XPS data on Co-Al catalyst are in the agreement with the conclusions on the Co-Al

hydrotalcite-like structure evolution during its calcination and reduction made in [9]. The Co-Al samples reduced at both 480 or 650°C contain the metallic Co species.

2. The following more or less amazing experimental results were obtained:
   2.1. The surface concentration of the Co^0 species for the Co-Al sample reduced at 480°C (as it is determined by XPS) is 2.5 times less than the amount of "accessible" Co^0 determined by the O_2 titration. The reduction at 650°C leads to an increase of the Co^0 surface concentration, the data of both XPS and the O_2 titration giving the same value of the Co^0 concentration increment.
   2.2. After reduction of the Co-Al sample, a photoemission at 75.2 eV (the Al 2p atomic level) appears. This value is by 0.7 eV higher than the Al 2p BE for the Al^{3+} cation of the Al_2O_3 oxide.
   2.3. The Co-Zn-Al and Co-Al samples reduced at 480°C do not chemisorb CO at 77 K.
   2.4. Carboxyls, monodentate carbonates, formates, and terminal carbonyls are detected in the all reduced samples during the CO treatment at elevated temperatures. For the samples reduced at 480°C, the absorption bands, ascribed to carbonyls, formates and monodentate carbonates are found to be shifted significantly to the lower frequencies.
3. The above listed observations, as well as the earlier obtained catalytic data force us to conclude on the existence of a strong metal–support interaction between the Co^0 nanoparticles and Al-containing oxide. The nature of the SMSI effect for the Co-Al catalysts consists plausibly in the formation of a $(Co_z)^{2y-w}$ $(Al_{2x}O_{3x+y-w}(OH)_w)^{w-2y}$ complex from the metallic nanoparticle and two-dimensional small Al-oxide clusters on its surface. This decreases the accessible Co^0 surface and causes the transfer of positive charge to the metallic particle giving $Co^{\delta+}$.
4. The suggested hypothesis may give an explanation for the "abnormal" catalytic properties of Co-Al catalysts in the CO hydrogenation, H_2–D_2 isotope exchange, CO oxidation, ethylene hydrogenation and other reactions, which were many times reported in literature. The SMSI $Co^{\delta+}$ seems not to be able to activate H_2, O_2, and C_2H_4 molecules at low and medium temperatures. The nature of interaction of SMSI $Co^{\delta+}$ with these molecules, as well as with CO, needs a further investigation.

References

[1] R. Oukaci, A.H. Singleton, J.A. Goodwin Jr., Appl. Catal. A: Gen. 186 (1999) 129.
[2] A. Lapidus, A. Krylova, V. Kazanskii, V. Borovikov, A. Zaitsev, J. Rathousky, A. Zukai, M. Jancalkowa, Appl. Catal. 73 (1991) 65.
[3] S. Vada, A. Hoff, E. Adnanes, D. Schanke, A. Holmen, Top. Catal. 2 (1995) 155.
[4] A.M. Hilmen, D. Schanke, A. Holmen, Catal. Lett. 38 (1996) 143.
[5] J. van de Loosdrecht, Preparation and Properties of Supported Fischer–Tropsch Catalysts, Ph.D. Thesis, Universiteit Utrecht, Utrecht, The Netherlands, 1995, Chapter 3.
[6] J. van de Loosdrecht, M. van der Haar, A.M. van der Kraan, A.J. van Dillen, J.W. Geus, Appl. Catal. A: Gen. 150 (1997) 365.
[7] L. Ji, J. Lin, H.C. Zeng, J. Phys. Chem. B 104 (2000) 1783.
[8] T. Komatsu, M. Fukui, T. Yashima, Stud. Surf. Sci. Catal. 101 (1996) 1095.
[9] A.A. Khassin, T.M. Yurieva, G.N. Kustova, I.S. Itenberg, M.P. Demeshkina, T.A. Kriger, L.M. Plyasova, G.K. Chermashentseva, V.N. Parmon, J. Mol. Catal. A: Chem. 168 (2001) 193.
[10] J.F. Moulder, W.F. Stickle, P.E. Sobol, K.D. Bomden, J. Chastain (Eds.), Handbook of X-Ray Photoelectron Spectroscopy, Perkin-Elmer, Eden Prairie, Minnesota, 1992.
[11] N.G. Farr, H.J. Griess, J. Electron Spectrosc. Rel. Phenom. 49 (1989) 293.
[12] G. Fierro, M.L. Jacono, M. Inversi, P. Porta, Top. Catal. 10 (2000) 39.
[13] A. Fritsch, P. Légaré, Surf. Sci. 186 (1987) 247.
[14] D.L. Cocke, E.D. Johnson, R.P. Merrill, Catal. Rev. Sci. Eng. 26 (1984) 163.
[15] N.S. McIntyre, M.G. Cook, Anal. Chem. 47 (1975) 2208.
[16] B.A. Sexton, A.E. Hughes, T.W. Turney, J. Catal. 97 (1986) 390.
[17] Z. Zsoldos, L. Guczi, J. Phys. Chem. 96 (1992) 9393.
[18] K.S. Chung, F.E. Massoth, J. Catal. 64 (1980) 320.
[19] B. Ernst, L. Hilaire, A. Kiennemann, Catal. Today 50 (1999) 413.
[20] A.M. Hilmen, D. Schanke, K.F. Hansen, A. Holmen, Appl. Catal. A 186 (1999) 169.
[21] R.L. Chin, D.M. Hercules, J. Phys. Chem. 86 (1982) 360.
[22] G. Busca, V. Lorenzelli, V.S. Escribano, R. Guidetti, J. Catal. 131 (1991) 167.
[23] A.A. Davydov. IR-Spectroscopy in the Chemistry of Oxide Surfaces, Nauka, Novosibirsk, 1984 (in Russian).
[24] G. Busca, R. Guidetti, V. Lorenzelli, J. Chem. Soc., Faraday Trans. 86 (1990) 989.

[25] A. Chiorino, E. Garrone, G. Ghiotti, New horizons in catalysis, in: Proceedings of the 7th International Congress on Catalysis, Part A, Tokyo, 1981, pp. 136–148.
[26] Y.A. Lokhov, A.A. Davydov, in: Catalytic Hydrocarbon Conversions, Irkutsk, 1980, pp. 36–41 (in Russian)
[27] M.J. Heal, E.C. Leisigang, R.G. Torrington, J. Catal. 51 (1978) 314.
[28] M.J. Dees, T. Schidi, Y. Iwazawa, V. Ponec, J. Catal. 124 (1990) 530.
[29] K. Sato, Y. Inoue, I. Kojima, E. Miyajaki, I. Yasumori, J. Chem. Soc., Faraday Trans. I 80 (1984) 841.
[30] K.R. Mohana, G. Spoto, A. Zecchina, J. Catal. 113 (1988) 466.
[31] S. Sun, N. Tsubaki, K. Fujimoto, Appl. Catal. A: Gen. 202 (2000) 121.
[32] C. Mirodatos, E.B. Pereira, A.G. Cobo, J.A. Dalmon, G.A. Martin, Top. Catal. 2 (1995) 183.
[33] J.P. Hindermann, G.J. Hutchings, A. Kiennemann, Catal. Rev. Sci. Eng. 35 (1) (1993) 1.
[34] A.B. Anderson, D.Q. Dowd, J. Phys. Chem. 91 (1987) 869.
[35] S.P. Mehandru, A.B. Anderson, Surf. Sci. 201 (1988) 345.
[36] P. Legare, F. Finck, R. Roche, G. Maire, Surf. Sci. 217 (1989) 167.
[37] G. Blyholder, J. Phys. Chem. 68 (1964) 2772.
[38] D. Drakova, G. Doyen, Surf. Sci. 226 (1990) 263.
[39] G. Kadinov, C. Bonev, S. Todorova, A. Palazov, J. Chem. Soc., Faraday Trans. 94 (1998) 3027.
[40] A.A. Khassin, T.M. Yurieva, V.N. Parmon, 2000, unpublished results.
[41] A.A. Khassin, V.V. Molchanov, M.P. Demeshkina, N.A. Zaitseva, I.S. Itenberg, G.N. Kustova, V.N. Parmon, L.M. Plyasova, G.K. Chermashentseva, T.M. Yurieva, R.A. Buyanov, Patent Application RU 2000132544, Priority Date 26 December 2000.